Modeling and Simulation of Upstream and Downstream Processes for Monoclonal Antibody Production

Morten Ryberg Wahlgreen [*] **Kristian Meyer** [**,***]
Tobias K. S. Ritschel [*] **Allan Peter Engsig-Karup** [*]
Krist V. Gernaey [**] **John Bagterp Jørgensen** [*,****]

[*] *Department of Applied Mathematics and Computer Science, Technical University of Denmark, DK-2800 Kgs. Lyngby, Denmark.*
[**] *Department of Chemical and Biochemical Engineering, PROSYS, Technical University of Denmark, DK-2800 Kgs. Lyngby, Denmark.*
[***] *MCT Bioseparation ApS, DK-2800 Kgs. Lyngby, Denmark.*
[****] *2-control ApS, DK-7400 Herning, Denmark.*

Abstract:
We present a numerical case study for modeling and simulation of upstream and downstream processes for monoclonal antibody (mAb) production. We apply a systematic and intuitive modeling methodology for an existing upstream process and downstream process. The resulting models are based on differential mass balances and kinetic expressions for the reactions and adsorption. Mass balances for the fedbatch reactor yield a model consisting of five ordinary differential equations (ODEs). The downstream process is conducted batchwise in a chromatographic column for capture of mAbs. Mass balances of the chromatographic column yield a system of partial differential equations (PDEs). The chromatographic model applies the nonlinear shrinking core adsorption isotherm model for transition between the mobile phase and the stationary phase. We apply a high-order spectral nodal continuous Galerkin scheme for spatial discretization of the chromatographic column, which result in a semi-discrete ODE formulation. The resulting simulation model, coupling the upstream and downstream processes in batchwise mAb production, can be used as a benchmark for numerical estimation, control and optimization studies.

Keywords: Monoclonal antibody production, fedbatch reactor, capture chromatography, shrinking core adsorption isotherm, process modeling.

1. INTRODUCTION

Monoclonal antibodies (mAbs) is a class of biopharmaceuticals representing the 6 top-selling biopharmaceutical products in 2017 (Walsh, 2018). There has been a huge increase in the sale of mAbs the previous years, and the yearly sale is expected to grow to 130-200 billion US dollars in 2022 (Grilo and Mantalaris, 2019). As such, new technology is needed to keep up with the increasing demand. The emerging need for huge mAb production has led to recent research in optimization of biotechnological processes for mAb production (Badr et al., 2021; Gomis-Fons et al., 2021). Most optimization is related to the development of mathematical models to support operation of the processes.

Modeling of upstream and downstream processes is well developed. However, often the model presentations are unnecessarily complicated and the chain rule is applied to the mass balance equations for fedbatch reactor models. Due to systematic and intuitive modeling and numerical considerations, we present the differential mass balance models in compact forms without using the chain rule. When used systematically, this modeling methodology has significant advantages in the modeling phase and in the numerical implementation phase. Additionally, the models presented in this paper are well-suited for model based optimization such as model predictive control (MPC). We intend to apply the developed models in model based optimization in future work and the key objective of the paper is to present a well-defined simulation model for batchwise mAb production, that can be used as a benchmark in numerical simulation, control and optimization studies.

This paper presents a numerical case study that combines modeling of an upstream and downstream process for mAb production. Fig. 1 presents an overview of the reactor (upstream process) and chromatographic column (downstream process). We apply the proposed modeling methodology to existing models for the upstream process and downstream process (Badr et al., 2021). We show that the methodology allows for easy modeling of fedbatch reactors for upstream processes. For the downstream process, the methodology results in a general compact model, which is even applicable for a wide range of reactions conducted in columns. We apply a high-order spectral nodal con-

[⋆] Corresponding author: J. B. Jørgensen (E-mail: jbjo@dtu.dk).

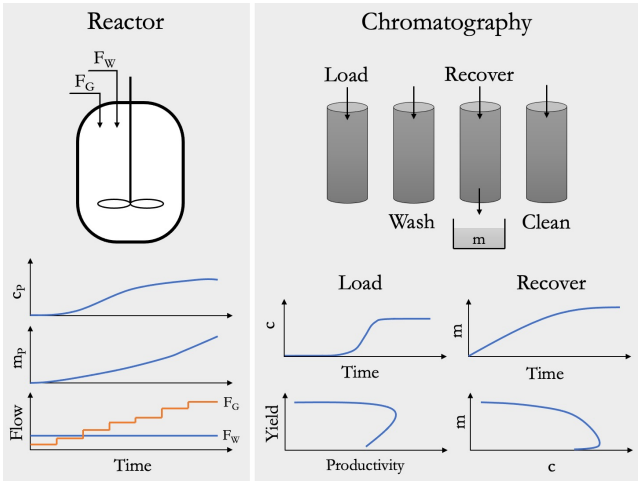

Fig. 1. Overview of the fedbatch reactor for fermentation and the chromatographic column operated batchwise.

tinuous Galerkin method (CGM) for space discretization of the chromatographic column. The method is based on Legendre polynomials on a Gauss-Lobatto grid. Recent results show that high order methods are very suitable for chromatographic processes as they outperform widely applied finite volume (FV) methods (Hørsholt et al., 2019a,b; Meyer et al., 2020). The chromatography model applies a nonlinear shrinking core adsorption isotherm model for transition between the mobile phase and the stationary phase. We demonstrate that the upstream and downstream model can be applied for simulation of mAb production and capture of mAbs respectively. The simulations of the chromatographic column show a trade-off between the productivity and yield of the column in the loading phase and a similar trade-off for captured mAbs and concentration of mAbs in the recovery phase. The trade-off indicates that optimization of the process can be advantageous.

The remaining part of the paper is organized as follows. Section 2 introduces the upstream process. Section 3 presents the downstream chromatographic process. Section 4 describes the applied methods for simulation. Section 5 presents the results. Section 6 presents the conclusion.

2. UPSTREAM PROCESS

We consider an upstream process for monoclonal antibody production conducted in a fedbatch reactor. The model was originally presented by Badr et al. (2021). We apply a systematic modeling methodology that is well-suited for modeling of the reactor in simulation, control, and optimization studies.

2.1 General model for fedbatch fermentation

The mass (mole) balance for well-mixed fedbatch fermentation, assuming constant and identical density, can be compactly states as (Ryde et al., 2021),

$$\frac{dV}{dt} = e^T F, \tag{1a}$$

$$\frac{dn}{dt} = C_{in} F + RV. \tag{1b}$$

Let $\mathcal{C}$ denote the set of components (molecules) and let $\mathcal{S}$ denote the set of inlet streams. $V \in \mathbb{R}$ is the medium volume, $e \in \mathbb{R}^{|\mathcal{S}|}$ is a vector of ones, $F \in \mathbb{R}^{|\mathcal{S}|}$ is the vector of flow rates in the inlet streams, $n \in \mathbb{R}^{|\mathcal{C}|}$ is the vector of mole numbers for each component in the reactor, $C_{in} \in \mathbb{R}^{|\mathcal{C}|\times|\mathcal{S}|}$ is a matrix of concentrations in the inlet streams, and $R \in \mathbb{R}^{|\mathcal{C}|}$ is the production rate vector. The concentration vector, $c \in \mathbb{R}^{|\mathcal{C}|}$, is

$$c = \frac{n}{V}. \tag{2}$$

Let $\mathcal{R}$ denote the set of reactions and let $S \in \mathbb{R}^{|\mathcal{R}|\times|\mathcal{C}|}$ denote the stoichiometric matrix for the considered reactions and components. $r \in \mathbb{R}^{|\mathcal{R}|}$ denotes the reaction rate vector. Specification of the stoichiometry and kinetics, i.e. S and $r = r(c)$, enables computation of the production rate,

$$r = r(c), \tag{3a}$$

$$R = S^T r, \tag{3b}$$

and completes the model.

In addition, the masses of the components, $m \in \mathbb{R}^{|\mathcal{C}|}$, may be of interest. It is computed by

$$m = M_w \odot n, \tag{4}$$

in which $\odot$ denotes elementwise multiplication and $M_w \in \mathbb{R}^{|\mathcal{C}|}$ is the molecular mass vector.

Remark. The model (1)-(4) is a general compact form, which is easy to implement. Additionally, the model equations reduce the actual modeling to specification of: $\mathcal{C}$, $\mathcal{R}$, $\mathcal{S}$, S, $r(c)$, C_{in}, F, and M_w, together with selection of initial conditions for (1).

Usual practice is to apply the chain rule to the mass balance equations (1) to represent the states as concentrations, c, rather than mole numbers, n. The result is a set of equations on the form,

$$\frac{dV}{dt} = e^T F, \tag{5a}$$

$$\frac{dc}{dt} = \left(C_{in} - ce^T\right)\frac{F}{V} + S^T r(c). \tag{5b}$$

However, we strongly recommend to apply (1) rather than (5), as (1) is more intuitive and application of the chain rule is only valid for an infinitely small, dt. As such, the formulations (1) and (5) are not numerical equivalent when solved with numerical solvers. The novelty of this work lies in the intuitive and compact formulation of the model (1).

2.2 Reaction stoichiometry and kinetics

We demonstrate the application of the general modeling methodology on a fedbatch fermentation model for mAb production (Badr et al., 2021). The model consists of four components,

$$\mathcal{C} = \{X, G, L, P\}, \tag{6}$$

where X is viable cells, G is glucose, L is lactate, and P is the product (mAbs), and five reactions,

$$\mathcal{R} = \{1, 2, 3, 4, 5\}. \tag{7}$$

The stoichiometry of the process is,

1. Cell production, $\alpha_{1,G}G + X \longrightarrow 2X$, r_1,
2. Cell death, $X \longrightarrow \alpha_{2,G}G$, r_2,
3. Cell maintenance, $\alpha_{3,G}G + X \longrightarrow X$, r_3,
4. Lactate production, $X \longrightarrow X + \alpha_{4,L}L$, r_4,
5. Product formation, $X \longrightarrow X + \alpha_{5,P}P$, r_5,

which can be represented by the stoichiometric matrix,

$$S = \begin{array}{c} \begin{matrix} \text{X} & \text{G} & \text{L} & \text{P} \end{matrix} \\ \begin{bmatrix} 1 & -\alpha_{1,G} & 0 & 0 \\ -1 & \alpha_{2,G} & 0 & 0 \\ 0 & -\alpha_{3,G} & 0 & 0 \\ 0 & 0 & \alpha_{4,L} & 0 \\ 0 & 0 & 0 & \alpha_{5,P} \end{bmatrix} \end{array} \begin{matrix} 1 \\ 2 \\ 3 \\ 4 \\ 5 \end{matrix} \tag{8}$$

The reaction rates, $r = [r_1\ r_2\ r_3\ r_4\ r_5]^T$, are,

$$r_1 = \mu_X(c_G, c_L)c_X, \qquad r_2 = \mu_D(c_G, c_L)c_X, \tag{9a}$$
$$r_3 = \mu_M c_X, \qquad r_4 = \mu_L c_X, \tag{9b}$$
$$r_5 = \mu_P c_X, \tag{9c}$$

where $\mu_X(c_G, c_L)$ and $\mu_D(c_G, c_L)$ are governed by Monod growth kinetics,

$$\mu_X = \mu_{max}\left(\frac{c_G}{K_G + c_G}\right)\left(\frac{K_L}{K_L + c_L}\right), \tag{10a}$$
$$\mu_D = k_d\left(\frac{c_L}{KD_L + c_L}\right)\left(\frac{KD_G}{KD_G + c_G}\right), \tag{10b}$$

and μ_M, μ_L, and μ_P are parameters for estimation.

2.3 Inlet streams

The reactor is operated in fedbatch mode with two inlets; 1) an inlet containing glucose and 2) a pure water inlet. We denote the flow rate of the water inlet and glucose inlet F_W and F_G, respectively. The concentration of glucose in the glucose inlet is denoted $c_{G,in}$. Hence,

$$C_{in} = \begin{bmatrix} 0 & 0 \\ c_{G,in} & 0 \\ 0 & 0 \\ 0 & 0 \end{bmatrix}, \quad F = \begin{bmatrix} F_G \\ F_W \end{bmatrix}, \quad \mathcal{S} = \{S_G, S_W\}. \tag{11}$$

The split into a water inlet and a substrate inlet makes the model affine in the inlet flow rates (Ryde et al., 2021). This is beneficial in optimization studies with the model.

3. DOWNSTREAM PROCESS

We consider a downstream chromatographic process for capture of the product P, i.e., mAbs. Similarly to the upstream process, the chromatographic model was originally presented by Badr et al. (2021). We point out that P does not distinguish between a product with deficiencies (from the reactor) and a product of higher quality (after the chromatographic process). We demonstrate that our systematic modeling methodology is applicable for the downstream process and results in a general model formulation for the capture chromatography process.

We assume that the process is conducted in a column with diameter, d_c, packed with a porous media with porosity, ε_c. We denote the total volume of the column, V, which allows for definition of the liquid volume, $V_l = \varepsilon_c V$, and the stationary volume, $V_s = (1 - \varepsilon_c)V$. The stationary volume, V_s, contains a number of spherical particles, N_p, with porosity, ε_p. The components of the model are the mobile phase concentration, $c(t, z)$, the pore phase concentration of free molecules, $c_p(t, z)$, and the pore phase concentration of bound molecules at different binding sites, $q(t, z)$. Additionally, we derive the general mass balance model under the following assumptions (Meyer, 2020),

- The column is homogeneously packed with particles.
- The particles are porous and spherical with constant diameter.
- The mobile phase density is constant.
- The viscosity is constant.
- Operational conditions are isothermal and adiabatic.
- No convection inside particles.
- No radial dispersion in the mobile phase.
- No diffusion in the pore phase.

3.1 General model for chromatography

The mass balances in the chromatography model are

$$\partial_t c = -\partial_z N + R, \tag{12a}$$
$$\partial_t c_p = R_p, \tag{12b}$$
$$\partial_t q = R_q, \tag{12c}$$

where (12a) is based on the mobile liquid volume and (12b)-(12c) are based on the pore volume in the particles. N denotes the flux in the mobile liquid phase and R denotes the transport (production) rate from the mobile liquid volume to the particle pore volume. Similarly, R_p and R_q denote the transport of molecules to the free and bound particle pore volume, respectively. We impose a convective flow inlet and outlet boundary condition,

$$N(t, 0) = vc_{in}(t), \tag{13a}$$
$$N(t, L) = vc(t, L), \tag{13b}$$

together with the following initial condition,

$$c(0, z) = c_0(z), \tag{14a}$$
$$c_p(0, z) = c_{p,0}(z), \tag{14b}$$
$$q(0, z) = q_0(z). \tag{14c}$$

The flux in the mobile liquid phase, N, is governed by advection (convection) and Fickian diffusion,

$$N = vc + J, \tag{15a}$$
$$J = -D\partial_z c, \tag{15b}$$

where v is the linear mobile liquid phase velocity in the column, J denotes Fick diffusion, and D is the diffusion coefficient.

The transport rate from the mobile liquid phase to the pore volume, R, is based on the open surface area of the particles. The open particle surface area per liquid volume in the chromatography column is

$$\begin{aligned} \phi_l &= \frac{N_p A_p \varepsilon_p}{V_l} = \frac{V_s}{V_p}\frac{A_p \varepsilon_p}{V_l} \\ &= \frac{(1 - \varepsilon_c)V}{(4/3)\pi(d_p/2)^3}\frac{4\pi(d_p/2)^2}{\epsilon_c V}\varepsilon_p = \frac{1 - \varepsilon_c}{\varepsilon_c}\varepsilon_p\frac{6}{d_p}, \end{aligned} \tag{16}$$

where V_p is the volume of a particle and d_p is the particle diameter. The open pore surface area per pore volume is

$$\phi_p = \frac{N_p A_p \varepsilon_p}{N_p V_p \varepsilon_p} = \frac{4\pi(d_p/2)^2}{(4/3)\pi(d_p/2)^3} = \frac{6}{d_p}. \tag{17}$$

Consequently, the transport rates are

$$R = -\phi_l r_p, \tag{18a}$$
$$R_p = \phi_p r_p + S_p^T r_q, \tag{18b}$$
$$R_q = S_q^T r_q, \tag{18c}$$

where $S = [S_p \ S_q]$ is the stoichiometric matrix for the transport rates (reaction rates) in the pores of the particle. r_p is the kinetic expression for the transport of molecules from the mobile liquid volume to the pore space of the particles. The transport, r_p, is given per open surface area. r_q is the kinetic expression for the transport of molecules in the particle pore spaces. These transport (reaction) rates can be expressed as

$$r_p = r_p(c, c_p), \tag{19a}$$
$$r_q = r_q(c_p, q). \tag{19b}$$

Remark. The model (12)-(19) is a general and compact formulation of the chromatographic column under the given assumptions. The mobile phase transport equation, (12a), can even be applied to model general reactions conducted in columns, e.g., reactions conducted in a plug-flow reactor.

Usual practice is to insert expressions (15)-(18) into (12) and get

$$\partial_t c = -v\partial_z c + D\partial_{zz} c - \frac{1-\epsilon_c}{\epsilon_c}\epsilon_p \frac{6}{d_c} r_p, \tag{20a}$$
$$\partial_t c_p = \frac{6}{d_c} r_p + S_q^T r_q, \tag{20b}$$
$$\partial_t q = S_q^T r_q, \tag{20c}$$

and even further insert selections of S_p, S_q, r_p, and r_q. We strongly recommend to apply the formulation (12) as it reduces the actual modeling of the chromatographic column to selection of production rates, R, R_p, and R_q, i.e., selection of S_p, S_q, r_p, and r_q, together with selection of inlet concentration, $c_{in}(t)$, and initial conditions (14). Also, the model (12)-(19) is a more intuitive formulation compared to (20). The novelty of this work is the introduction of the very compact model (12).

3.2 Shrinking core adsorption isotherm

We demonstrate the general modeling methodology on a capture chromatography model (Badr et al., 2021). The model applies a shrinking core adsorptions isotherm, which has previously been proposed as a valid model for modeling of chromatographic processes (Baur et al., 2016a,b). As such, we select the quantities, S_p, S_q, r_p, and r_q based on the shrinking core adsorption model.

The kinetic expression for the transport rate from the mobile phase to the pore space of the particles are

$$r_p = k(c - c_p), \tag{21}$$

where k is the transport coefficient.

The shrinking core adsorption isotherm assumes two sites for adsorption, $q = [q_1, q_2]^T$. The stoichiometry of the transport in the pores of the particles is

$$S = [S_p \ S_q] = \left[\begin{array}{c|cc} -1 & 1 & 0 \\ -1 & 0 & 1 \end{array}\right], \tag{22}$$

and the corresponding kinetic expression is

$$r_q = \begin{bmatrix} k_{A,1}\left(c_p(q_{\text{sat}} - q_1) - \dfrac{q_1}{k_{eq}}\right) \\ k_{A,2}\left(c_p(q_1 - q_2) - \dfrac{q_2}{k_{eq}}\right) \end{bmatrix}, \tag{23}$$

where $k_{A,1}$ and $k_{A,2}$ are the adsorption rate constants for each site, q_{sat} is the saturation capacity, and k_{eq} is the equilibrium constant of the adsorption process.

The transport coefficient, k, is given as a combination of the two site contributions as,

$$\frac{1}{k} = \frac{1}{k_F} + \frac{1}{k_S}, \tag{24}$$

where k_F is the film transfer coefficient and k_S is the pore transfer coefficient. The two transfer coefficients can be computed as,

$$k_F = \frac{1.09 u_{sf}}{\varepsilon_c}, \tag{25}$$
$$k_S = D_s \frac{(1-\alpha)^{1/3}}{1-(1-\alpha)^{1/3}}, \tag{26}$$

where D_s is a fitting parameter, $u_{sf} = v\varepsilon_c$ is the superficial velocity, and

$$\alpha = \frac{q_1}{q_{\text{sat}}} \frac{1/k_{eq} + c_{in}}{c_{in}}. \tag{27}$$

The combination of the shrinking core model and the general PDE for chromatographic processes, (12), results in nonlinear chromatography described by a nonlinear PDE.

3.3 Loading of column

We select a rectangular pulse inlet boundary condition,

$$c_{in}(t) = \begin{cases} 0, & t < t_1 \\ c_f, & t_1 \le t \le t_2 \\ 0, & t > t_2 \end{cases}, \tag{28}$$

where c_f is the feed concentration, t_1 is the start of the loading phase, and t_2 is the end of the loading phase.

3.4 Yield and productivity in loading phase

The capture chromatography process has four phases as illustrated in Fig. 1; 1) loading of column, 2) washing of column, 3) recovery of product, and 4) cleaning of column. We assume constant operation time for phase 2-4 and denote the time in those phases t_c. The time in phase 2-4 is given as $t_c = 21$CV (column volumes) (Badr et al., 2021), i.e., the time it takes the liquid to run through the column 21 times. As such, we consider the yield, Y, and the productivity, Q, of the column,

$$Y(t) = \frac{m}{m_{in}}, \tag{29}$$
$$Q(t) = \frac{m}{t + t_c}, \tag{30}$$

where $m = m(t)$ [g] is the total accumulated mass of captured mAbs in the column at time t, and $m_{in} = m_{in}(t)$ is the total accumulated mass of mAbs injected to the column at time t.

Table 1. Parameters for reactor model.

Parameter	Value	Unit
K_G	0.0	[mmol/L]
K_L	7.10	[mmol/L]
KD_G	1.54	[mmol/L]
KD_L	0.0	[mmol/L]
μ_{max}	5.17×10^{-2}	[h^{-1}]
k_d	2.32×10^{-2}	[h^{-1}]
μ_M, μ_L, μ_P	1.0	[h^{-1}]
$\alpha_{1,G}$	7.52×10^{-10}	[mmol/cell]
$\alpha_{2,G}$	$= \alpha_{1,G}$	[mmol/cell]
$\alpha_{3,G}$	82.3×10^{-12}	[mmol/cell]
$\alpha_{4,L}$	2.76×10^{-11}	[mmol/cell]
$\alpha_{5,P}$	5.45×10^{-15}	[mmol/cell]
M_P	$\approx 0.15 \times 10^3$	[g/mmol]
$c_{G,in}$	130	[g/L]
M_G	0.180156	[g/mmol]

Table 2. Parameters for chromatographic process.

Parameter	Value (Load/Recover)	Unit
L	2.0	[cm]
d_c	15.0	[cm]
ε_c	0.36	[-]
d_p	85.0×10^{-4}	[cm]
ε_p	0.52	[-]
u_{sf}	1.33	[cm/min]
D	5.0×10^3	[cm^2/min]
c_f	2.4847 / 0.0	[g/L]
t_1	0 / 0	[min]
t_2	180 / 30	[min]
D_s	2.23×10^{-3}	[cm/min]
$k_{A,1}$	6.77×10^4	[min^{-1}]
$k_{A,2}$	3.18×10^4	[min^{-1}]
k_{eq}	61.47 / 0.001	[L/g]
q_{sat}	69.10	[g/L]
t_c	45.36	[min]

4. SIMULATION

The reactor model (1) consists of a system of non-stiff ODEs, which we solve in Matlab with `ode45`.

We apply a high-order CGM for spatial discretization of the chromatography model (12) (Hesthaven and Warburton, 2008). We solve the resulting system of semi-discrete ODEs in Matlab with an implicit variable step-size solver, `ode15s`, as the spatially discretized system is stiff.

5. RESULTS

This section presents simulation results for both models.

5.1 Upstream simulation

We simulate the reactor model (1). Table 1 presents the model parameters (Badr et al., 2021). Fig. 2 presents the simulation. The final concentration of the product, mAbs, is 2.48 [g/L], which we apply as inlet concentration, c_f, for the capture chromatography process.

5.2 Downstream simulation

We simulate the loading phase and recovery phase of the capture chromatographic model (12). Table 2 provides the parameters for the simulation adapted from Badr et al. (2021). Fig. 3 presents the result. Fig. 3a and

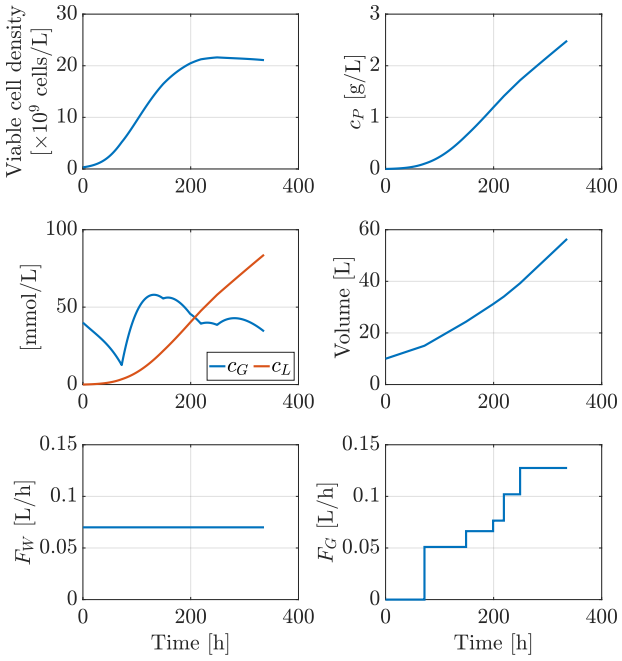

Fig. 2. Simulation of upstream process. States at the final time: $c_P = 2.48$ [g/L], $V = 56.44$ [L], and $m_P = 140.25$ [g].

3b presents the loading phase results, where we observe a breakthrough in the column and a trade-off between yield and productivity of the column. Fig. 3c and 3d presents the recovery phase results, where we observe a trade-off between recovered mAb mass and recovered mAb concentration.

6. CONCLUSION

The paper presents a systematic methodology for upstream and downstream process modeling. The methodology simplifies the model presentation and reduces the actual modeling to selection of stoichiometric matrices and reaction kinetics for both upstream and downstream processes. We demonstrate the modeling methodology on an existing model for mAb production in a fedbatch reactor and a chromatography model for capture of mAbs. The upstream process model is a five component ODE, while the downstream process is a nonlinear PDE. The chromatographic model applies a nonlinear shrinking core adsorption isotherm to model the transition between the mobile phase and the stationary phase in the chromatographic column. We discretize the nonlinear PDE in space with a high-order spectral continuous Galerkin scheme that can be expanded to a multi-element spectral scheme for better resolution and scalability. Simulation of the upstream and downstream processes shows that the modeling methodology works as intended. In particular, the chromatographic process results in a Pareto front for the yield and productivity in the loading phase and a Pareto front for the concentration of mAbs and captured mAbs in the recovery phase.

The proposed modeling methodology is well-suited for model-based optimization of the upstream and downstream processes.

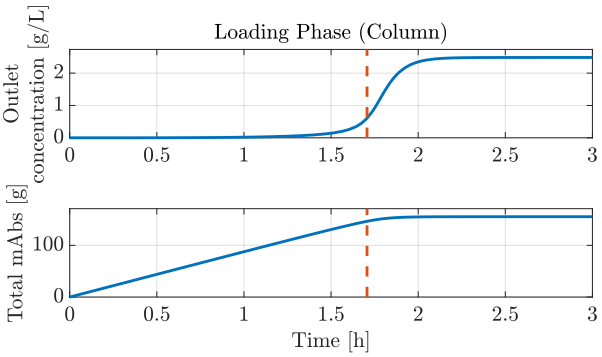

(a) Loading phase of the column. 1) The mobile phase concentration in the outlet of the column, where a breakthrough is observed, and 2) The total mAbs captured in the column. The red dotted line indicates a possible operating point for ending the loading phase.

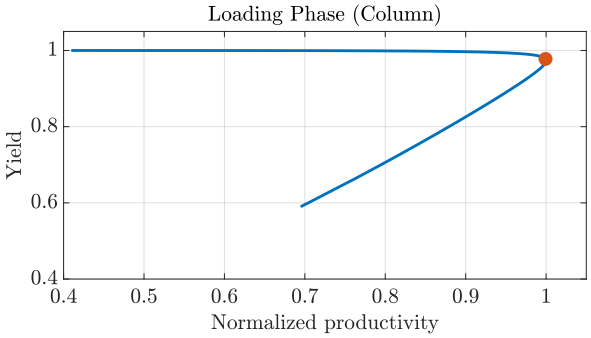

(b) The normalized productivity vs. the yield of the loading phase. The plot forms a Pareto front. The red dot indicates the operating point indicated in Fig. 3a.

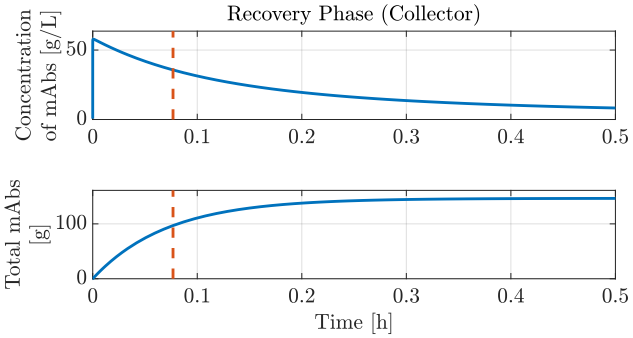

(c) Recovery phase of the column after the loading operation indicated on Fig. 3a. 1) The concentration of mAbs in the collector, and 2) The total mAbs in the collector. The red dotted line indicates a possible operating point for ending the recovery phase.

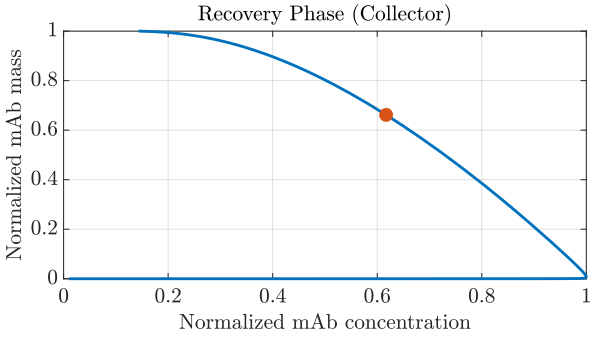

(d) Normalized concentration vs. normalized total product of the recovery phase. The plot forms a Pareto front. The red dot indicates the operating point indicated in Fig. 3c.

Fig. 3. Simulation of loading phase and recovery phase of the chromatographic column.

REFERENCES

Badr, S., Okamura, K., Takahashi, N., Ubbenjans, V., Shirahata, H., and Sugiyama, H. (2021). Integrated design of biopharmaceutical manufacturing processes: Operation modes and process configurations for monoclonal antibody production. *30th European Symposium on Computer Aided Process Engineering (ESCAPE)*, 153, 107422.

Baur, D., Angarita, M., Müller-Späth, T., and Morbidelli, M. (2016a). Optimal model-based design of the twin-column CaptureSMB process improves capacity utilization and productivity in protein A affinity capture. *Biotechnology Journal*, 11(1), 135–145.

Baur, D., Angarita, M., Müller-Späth, T., Steinebach, F., and Morbidelli, M. (2016b). Comparison of batch and continuous multi-column protein A capture processes by optimal design. *Biotechnology Journal*, 11(7), 920–931.

Gomis-Fons, J., Yamanee-Nolin, M., Andersson, N., and Nilsson, B. (2021). Optimal loading flow rate trajectory in monoclonal antibody capture chromatography. *Journal of Chromatography A*, 1635, 461760.

Grilo, A.L. and Mantalaris, A. (2019). The Increasingly Human and Profitable Monoclonal Antibody Market. *Trends in Biotechnology*, 37(1), 9–16.

Hesthaven, J.S. and Warburton, T. (2008). *Nodal Discontinuous Galerkin Nethods: Algorithms, Analysis, and Applications*, volume 54. Springer.

Hørsholt, A., Christiansen, L.H., Meyer, K., Huusom, J.K., and Jørgensen, J.B. (2019a). Spatial Discretization and Kalman Filtering for Ideal Packed-Bed Chromatography. *18th European Control Conference (ECC)*, 2356–2361.

Hørsholt, A., Christiansen, L.H., Ritschel, T.K., Meyer, K., Huusom, J.K., and Jørgensen, J.B. (2019b). State and Input Estimation of Nonlinear Chromatographic Processes. *Conference on Control Technology and Applications (CCTA)*, 1030–1035.

Meyer, K. (2020). *Advanced simulation of preparative chromatography processes*. Ph.D. thesis, Technical University of Denmark.

Meyer, K., Leweke, S., von Lieres, E., Huusom, J.K., and Abildskov, J. (2020). Chromatech: A discontinuous Galerkin spectral element simulator for preparative liquid chromatography. *Computers and Chemical Engineering*, 141, 107012.

Ryde, T.E., Wahlgreen, M.R., Nielsen, M.K., Hørsholt, S., Jørgensen, S.B., and Jørgensen, J.B. (2021). Optimal Feed Trajectories for Fedbatch Fermentation with Substrate Inhibition Kinetics. *IFAC-PapersOnline*, 54(3), 318–323.

Walsh, G. (2018). Biopharmaceutical benchmarks 2018. *Nature Biotechnology*, 36(12), 1136–1145.